same position as found in this work (see Fig. 3). The octahedral vacancy in the Inoue & Yamashita map has a charge less than or equal to 0·26 e $Å^{-3}$. The agreement with the map found in this work seems quite acceptable.

This research was supported by NSF Grant MPS-74-17592. A grant of computer time from the Mellon Institute NMR Facility for Biomedical research (NIH Grant RR00292) is appreciated. The author also acknowledges help from Dr John Bentley in converting the least-squares program for analysis of Be to the time-sharing system on the IBM 360 at Carnegie–Mellon University.

References

BENTLEY, J. J. & STEWART, R. F. (1976). *Acta Cryst.* A**32**, 910–914.
BROWN, P. J. (1972). *Phil. Mag.* **26**, 1377–1394.
CLEMENTI, E. (1965). *IBM J. Res. Dev.* **9**, 2 (Suppl.).
CLEMENTI, E. & RAIMONDI, D. L. (1963). *J. Chem. Phys.* **38**, 2686–2689.
CROMER, D. T. & LIBERMAN, D. (1970). *J. Chem. Phys.* **53**, 1891–1898.
HAMILTON, W. (1965). *Acta Cryst.* **18**, 502–510.
INOUE, S. T. & YAMASHITA, J. (1973). *J. Phys. Soc. Japan*, **35**, 677–683.
MACKAY, K. J. H. & HILL, N. A. (1963). *J. Nucl. Mater.* **8**, 263–264.
STEWART, R. F. (1976). *Acta Cryst.* A**32**, 565–574.

Acta Cryst. (1977). A**33**, 38–45

Errors in Atomic Parameters and in Electron Density Distributions Due to Thermal Diffuse Scattering of X-rays

BY R. B. HELMHOLDT* AND AAFJE VOS

Laboratorium voor Structuurchemie, Rijksuniversiteit Groningen, Zernikelaan, Paddepoel, Groningen, The Netherlands

(*Received* 11 *May* 1976; *accepted* 12 *June* 1976)

Errors in X-ray diffraction intensities due to first-order thermal diffuse scattering (TDS) have been calculated from the elastic constants of the crystal. Formulae given in the literature were generalized in such a way that they include quantum effects and zero-point vibrations. It is shown that, within the approximations used, the influence of quantum effects and zero-point vibrations is negligible above 5K if ordinary measuring conditions are applied. For $C_6H_5COCOC_6H_5$ and $NH_4HC_2O_4.\frac{1}{2}H_2O$ an estimate is made of the influence of TDS intensity errors on least-squares parameters and electron density distributions at 15, 110 and 293K. A critical discussion of the long-wave method used is given.

Introduction

In earlier papers (*e.g.* Göttlicher, 1968; Willis, 1969) the errors in X-ray diffraction intensities due to thermal diffuse scattering (TDS) have been discussed and estimates of their influence on the parameters of the atoms have been given. However, estimates of the errors in the parameters and electron density distribution due to neglect of TDS corrections, have not yet been made for crystals containing molecules with low symmetry. In the present paper we discuss the errors for dibenzoyl (DBZ; $C_6H_5COCOC_6H_5$) and ammonium hydrogen oxalate hemihydrate (AHO; $NH_4HC_2O_4.\frac{1}{2}H_2O$). The first is soft with respect to elasticity, for the second the elasticity is higher and more anisotropic. A list of symbols used in this paper is given in Table 1.

The formulae used in the present paper contain a number of approximations among which the following are of fundamental importance: (*a*) the atoms are assumed to vibrate (pseudo)harmonically, (*b*) second and higher order phonon scattering is neglected and only acoustic modes are considered, (*c*) the frequency of an acoustic mode is assumed to be proportional to its wave vector, thus

$$\omega_j(\mathbf{g}) = 2\pi v_j(\hat{\mathbf{e}})g\,, \qquad (1)$$

and for expressions of type $\exp(-2\pi i\mathbf{g}\,.\,\mathbf{a}_i)$ we use the approximation

$$\exp(-2\pi i\mathbf{g}\,.\,\mathbf{a}_i) = 1 - 2\pi i\mathbf{g}\,.\,\mathbf{a}_i\,. \qquad (2)$$

This corresponds to the method of long waves (Born & Huang, 1968, Ch. V) which can be used for $g \ll a^i$.

Theory

TDS distribution around a reflexion **H**

In the pseudo-harmonic approximation the distribution $I_1(\mathbf{S})$ of the first-order diffuse scattering around a point **H** in reciprocal space is given by (Cochran, 1963)

* Present address: Reactor Centrum Nederland, Westerduinweg 3, Petten (NH), The Netherlands.

Table 1. *List of symbols not defined explicitly in the text*

$\mathbf{a}_l$	Unit-cell parameters
$\mathbf{a}^l$	Reciprocal cell vectors ($\mathbf{a}_l \cdot \mathbf{a}^j = \delta_l^j$)
λ	Wavelength of X-rays
$\mathbf{s}_0, \mathbf{s}$	Wave vector of incident, and scattered, X-rays ($s_0 = s = 1/\lambda$)
2θ	Scattering angle
$\mathbf{S}$	Scattering vector [$S = (2 \sin\theta)/\lambda$]
$\mathbf{H}$	Vector to reciprocal lattice point
$\mathbf{r}(\kappa)$	Position vector of atom κ in the unit cell
$f(\kappa, \mathbf{S})$	X-ray scattering factor of atom κ (including temperature factor)
$F(\mathbf{H})$	Structure factor for reflexion $\mathbf{H}$
$I_0^B(\mathbf{H})$	Bragg intensity
V	Volume of unit cell
m	Mass of unit cell
ϱ	Density of crystal
N	Number of unit cells
T	Temperature in degrees Kelvin
h	Planck's constant
$\hbar$	$h/2\pi$
k	Boltzmann's constant
c_{ijmk}	Element of elastic tensor
$(A^{-1})_{ik}$	ikth element of the inverse Christoffel matrix (Wooster, 1962)
$\hat{\mathbf{p}}$	Unit vector parallel to $\mathbf{H}$
$\mathbf{g}$	Wave vector of elastic wave. Only the three acoustic modes are considered for each $\mathbf{g}$
$\hat{\mathbf{e}}$	Unit vector parallel to $\mathbf{g}$
$\omega_j(\mathbf{g})$	Circular frequency of mode $(j, \mathbf{g})$
$E_j(\mathbf{g})$	Energy of mode $(j, \mathbf{g})$
$\hat{\mathbf{U}}_j(\kappa\mathbf{g})$	Normalized amplitude vector describing the displacement of atom κ due to mode $(j, \mathbf{g})$
$\hat{\mathbf{u}}_j(\hat{\mathbf{e}})$	Polarization vector of mode j for direction $\hat{\mathbf{e}}$
$v_j(\hat{\mathbf{e}})$	Velocity of mode j for the direction $\hat{\mathbf{e}}$
$I_1(\mathbf{H})$	First-order TDS intensity for reflexion $\mathbf{H}$
$\alpha(\mathbf{H})$	Net first-order TDS intensity for reflexion $\mathbf{H}$ in units $I_0^B(\mathbf{H})$
$\alpha_1(\mathbf{H})$	Total first-order TDS intensity for reflexion $\mathbf{H}$ in units $I_0^B(\mathbf{H})$
$\alpha_1'(\mathbf{H})$	TDS background for reflexion $\mathbf{H}$ in units $I_0^B(\mathbf{H})$
$G_j(\mathbf{S})$	Structure factor for first-order phonon scattering
$\Phi(Y_j)$	Debye integral
$F(Y_j)$	Correction factor for quantum effects and zero-point vibration.

$$I_1(\mathbf{S}) = \frac{4\pi^2 S^2 N}{m} \sum_{j=1}^{3} \frac{E_j(\mathbf{g})}{\omega_j^2(\mathbf{g})} |G_j(\mathbf{S})|^2 \qquad (3)$$

where

$$SG_j(\mathbf{S}) = \mathbf{S} \cdot \sum_{\kappa} \hat{\mathbf{U}}_j(\kappa\mathbf{g}) f(\kappa, \mathbf{S}) \exp[2\pi i \mathbf{H} \cdot \mathbf{r}(\kappa)], \qquad (4)$$

$\mathbf{S} = \mathbf{H} - \mathbf{g}$ and $j = 1, 2, 3$ if acoustic modes are considered only.

Within the framework of the long-wave method [see (1) and (2)] the normalized wave amplitudes $\hat{\mathbf{U}}_j(\kappa\mathbf{g})$ do not depend on κ and on the value of $\mathbf{g}$ (Born & Huang, 1968, § 26) so that we can take

$$\hat{\mathbf{U}}_j(\kappa\mathbf{g}) = \hat{\mathbf{u}}_j(\hat{\mathbf{e}}) . \qquad (5)$$

By use of (5) and (1) and the assumptions $|\mathbf{S}| = |\mathbf{H}|$ and $f(\mathbf{S}) = f(\mathbf{H})$, which is justified for all (higher order) reflexions for which the effect of TDS on the intensity is not negligible we obtain

$$I_1(\mathbf{H} \pm \mathbf{g}) = \frac{NH^2 |F(\mathbf{H})|^2}{m} \sum_{j=1}^{3} \frac{E_j(\mathbf{g})}{v_j^2(\hat{\mathbf{e}}) g^2} [\hat{\mathbf{u}}_j(\hat{\mathbf{e}}) \cdot \hat{\mathbf{p}}]^2 \qquad (6)$$

where

$$I_1(\mathbf{H} \pm \mathbf{g}) = \tfrac{1}{2}[I_1(\mathbf{H} + \mathbf{g}) + I_1(\mathbf{H} - \mathbf{g})] .$$

In units of the Bragg intensity $I_0^B(\mathbf{H}) = N|F(\mathbf{H})|^2/V$ (Cochran, 1963, p. 18) and with $m = \varrho V$ this intensity is equal to

$$\alpha_1(\mathbf{H} \pm \mathbf{g}) = I_1(\mathbf{H} \pm \mathbf{g})/I_0^B(\mathbf{H}) = \frac{H^2}{g^2} \sum_{j=1}^{3} E_j(\mathbf{g}) \frac{[\hat{\mathbf{u}}_j(\hat{\mathbf{e}}) \cdot \hat{\mathbf{p}}]^2}{\varrho v_j^2(\hat{\mathbf{e}})} . \qquad (7)$$

Integration for each direction of $\mathbf{g}$

The total TDS function, $\alpha_1(\mathbf{H})$, for a reflexion $\mathbf{H}$ is given by integration of $\alpha_1(\mathbf{H} + \mathbf{g})$ over the volume in reciprocal space swept out by the scan. If symmetrical scans are taken the TDS contributions at $\mathbf{H} + \mathbf{g}$ and $\mathbf{H} - \mathbf{g}$ can be considered together, so that the further integration can be restricted to half the volume. Difficulties concerning the singularity of (7) at the reciprocal lattice point $\mathbf{H}$ ($g = 0$) are avoided by doing the integration analytically for each direction of the vectors $\mathbf{g}$ (a similar procedure has been followed by Walker & Chipman, 1970). To this end the volume is divided into pyramids, each with its apex at the endpoint of $\mathbf{H}$. The contribution of the pyramids around $\mathbf{g}$ and $-\mathbf{g}$, each having a solid angle $\mathrm{d}\eta(\mathbf{g})$ and height G, is given by

$$\alpha_1(\mathbf{H}, \mathbf{g}) \mathrm{d}\eta(\mathbf{g}) = 2 \int_0^G \alpha_1(\mathbf{H} \pm \mathbf{g}) g^2 \mathrm{d}g \mathrm{d}\eta(\mathbf{g}) . \qquad (8)$$

From (8), (7) and (1) and the relation

$$E_j(\mathbf{g}) = (\{\exp[hv_j(\hat{\mathbf{e}})g/kT] - 1\}^{-1} + 0{\cdot}5) hv_j(\hat{\mathbf{e}}) g \qquad (9)$$

for the energy of the modes, we obtain

$$\alpha_1(\mathbf{H}, \mathbf{g}) \mathrm{d}\eta(\mathbf{g}) = 2hH^2 \sum_{j=1}^{3} \frac{[\hat{\mathbf{u}}_j(\hat{\mathbf{e}}) \cdot \hat{\mathbf{p}}]^2}{\varrho v_j^2(\hat{\mathbf{e}})} v_j(\hat{\mathbf{e}}) \mathrm{d}\eta(\mathbf{g}) \times \int_0^G (\{\exp[hv_j(\hat{\mathbf{e}})g/kT] - 1\}^{-1} + 0{\cdot}5) g \mathrm{d}g . \qquad (10)$$

The integral in (10) is familiar from the theory of specific heat (Debye, 1914). By making use of the function

$$\Phi(Y_j) = \frac{1}{Y_j} \int_0^{Y_j} \frac{y_j \mathrm{d}y_j}{\exp(y_j) - 1}$$

tabulated in *International Tables for X-ray Crystallography* (1959), (10) can be written as

$$\alpha_1(\mathbf{H}, \mathbf{g}) \mathrm{d}\eta(\mathbf{g}) = 2kTH^2 G \sum_{j=1}^{3} \frac{[\hat{\mathbf{u}}_j(\hat{\mathbf{e}}) \cdot \hat{\mathbf{p}}]^2}{\varrho v_j^2(\hat{\mathbf{e}})} \mathrm{d}\eta(\mathbf{g}) F(Y_j) \qquad (11)$$

with $F(Y_j) = \Phi(Y_j) + 0{\cdot}25 Y_j$, $y_j = hv_j(\hat{\mathbf{e}})g/kT$ and $Y_j = hv_j(\hat{\mathbf{e}})G/kT$. For $Y_j \to 0$ or $kT \gg hv_j(\hat{\mathbf{e}})G$ and $E_j(\mathbf{g}) = kT$, $\lim F(Y_j) = 1$. Hence the factor $F(Y_j)$ can be considered as the correction for quantum effects and zero-point vibration.

Integration over the different directions; TDS background

The volume swept out by the scan is a parallelepiped, to a good approximation (Fig. 1). For symmetrical scans the endpoint M of $\mathbf{H}$ corresponds to its centre. The three independent boundary planes of the parallelepiped are indicated by the index l ($l=1,2,3$) and the distances of M to the planes by d_l. The basal planes of the pyramids are formed by dividing each plane l into a number of parallelograms with surface ΔO_l. The positions of the parallelograms are given by the indices n and q and the angle between the vector $\mathbf{g}(l,n,q)$ and the normal to l is given by β_{lnq}. For pyramid l,n,q the solid angle is thus

$$d\eta(\mathbf{g})=(\Delta O_l \cos\beta_{lnq})/G^2 = (\Delta O_l \cos^2\beta_{lnq})/(Gd_l)\,. \quad (12)$$

The total fractional contribution $\alpha_1(\mathbf{H})$ of the TDS to the reflexion $\mathbf{H}$ is obtained by summation over all the pyramids, which gives by use of (11) and (12)

$$\alpha_1(\mathbf{H})=2kTH^2 \sum_{l=1}^{3} \frac{\Delta O_l}{d_l} \times \sum_{n=1}^{N_l}\sum_{q=1}^{Q_l} \cos^2\beta_{lnq} \left\{ \sum_{j=1}^{3} \frac{[\hat{\mathbf{u}}_j(\hat{\mathbf{e}})\cdot\hat{\mathbf{p}}]^2}{\varrho v_j^2(\hat{\mathbf{e}})} F(Y_j) \right\}_{lnq}. \quad (13)$$

Fig. 2 shows that the fractional error $\alpha(\mathbf{H})$ in the Bragg intensity due to TDS is given by

$$\alpha(\mathbf{H})=\alpha_1(\mathbf{H})-\alpha_1'(\mathbf{H}) \quad (14)$$

where $\alpha_1'(\mathbf{H})$ is the fractional TDS background which for a symmetrical scan is given by

$$\alpha_1'(\mathbf{H})=L\alpha_1(\mathbf{H},\omega_E)\,. \quad (15)$$

$\alpha_1(\mathbf{H},\omega_E)$ is the integration of (7) over the reflecting section of reciprocal space seen by the counter for position ω_A (or ω_B) of the crystal. L is the perpendicular distance between the sections at ω_A and ω_B. The result of this numerical integration can be written as

$$\alpha_1'(\mathbf{H})=LH^2\Delta O(\omega_E) \sum_{n=1}^{N}\sum_{q=1}^{Q} \frac{1}{g_{nq}^2} \times \left\{ \sum_{j=1}^{3} \frac{[\hat{\mathbf{u}}_j(\hat{\mathbf{e}})\cdot\hat{\mathbf{p}}]^2}{\varrho v_j^2(\hat{\mathbf{e}})} E_j(\mathbf{g}) \right\}_{nq}. \quad (16)$$

Simplification of the formulae by neglect of quantum effects

In the literature $\alpha_1(\mathbf{H})$ and $\alpha_1'(\mathbf{H})$, or analogous expressions in non-integrated form, are given as functions of the elastic constants c_{ilmk} of the crystal. It is easy to see that with neglect of quantum effects, thus for $F(Y_j)=1$ and $E_j(\mathbf{g})=kT$, and by use of the relation (Wooster, 1962)

$$\sum_{j=1}^{3} \frac{[\hat{\mathbf{u}}_j(\hat{\mathbf{e}})\cdot\hat{\mathbf{p}}]^2}{\varrho v_j^2(\hat{\mathbf{e}})} = \sum_{i=1}^{3}\sum_{k=1}^{3} p_i p_k (A^{-1})_{ik} \quad (17)$$

with

$$A_{ik}=\sum_{l=1}^{3}\sum_{m=1}^{3} c_{ilmk}\hat{e}_l\hat{e}_m\,,$$

(13) and (16) reduce to the familiar forms

$$\alpha_1(\mathbf{H})=2kTH^2 \sum_{l=1}^{3} \frac{\Delta O_l}{d_l} \sum_{n=1}^{N_l}\sum_{q=1}^{Q_l} \cos^2\beta_{lnq} \times \left[\sum_{i=1}^{3}\sum_{k=1}^{3} p_i p_k (A^{-1})_{ik} \right]_{lnq} \quad (13a)$$

and

$$\alpha_1'(\mathbf{H})=kTLH^2\Delta O(\omega_E) \times \sum_{n=1}^{N}\sum_{q=1}^{Q} \frac{1}{g_{nq}^2} \left[\sum_{i=1}^{3}\sum_{k=1}^{3} p_i p_k (A^{-1})_{ik} \right]_{nq}. \quad (16a)$$

Computer programs

Two computer programs have been written in Fortran: *TDS*1 based on (13*a*) and (16*a*) and *TDS*2 based on

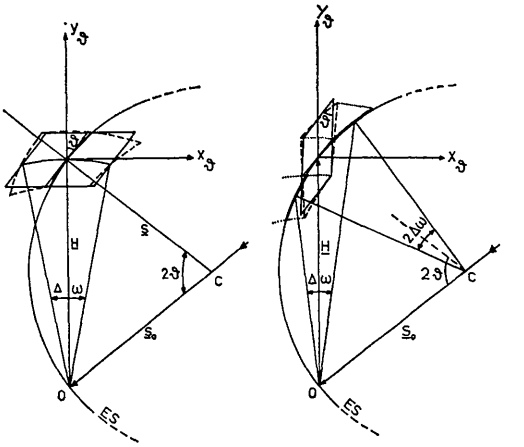

Fig. 1. Volume swept out by the scan; $\Delta\omega$ is drawn on an enlarged scale. (*a*) ω-scan, (*b*) $\theta/2\theta$-scan. --- Boundary of section through real volume, — boundary of volume used. Axes X_θ and Y_θ are indicated, $\mathbf{Z}_\theta=\mathbf{X}_\theta\times\mathbf{Y}_\theta$.

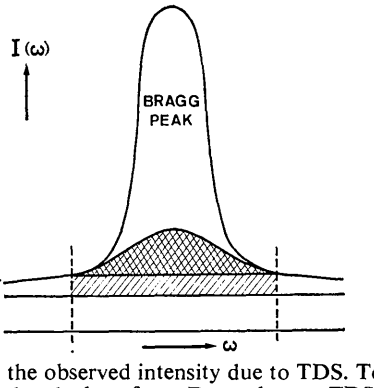

Fig. 2. Error in the observed intensity due to TDS. Total TDS contribution: hatched surface. Error due to TDS: doubly hatched surface. TDS background: singly hatched surface. The values of the surfaces, in units of the Bragg intensity $I_0^B(\mathbf{H})$, are given by $\alpha_1(\mathbf{H})$, $\alpha_1(\mathbf{H})$ and $\alpha_1'(\mathbf{H})$.

(13) and (16). Calculations can be carried out for ω and $\theta/2\theta$ scans. The volume of reciprocal space swept out by the scan is determined in the axial system $X_\theta Y_\theta Z_\theta$ of Fig. 1. A section of the volume is outlined in the figure. Numerically the volume is defined as

$$\begin{aligned}
\omega \text{ scan:} \quad & |x| \le 0{\cdot}5\ H|\Delta\omega| + y \tan\theta \\
& |y| \le T\cos\theta/(2\lambda R) \\
& |z| \le V/(2\lambda R)\ . \\
\theta/2\theta \text{ scan:} \quad & |x| \le T\sin\theta/(2\lambda R) \\
& |y| \le 0{\cdot}5\ H|\Delta\omega| \text{ cotan } \theta + x \text{ cotan } \theta \\
& |z| \le V/(2\lambda R)\ ,
\end{aligned}$$

T being the width and V the height of the counter slit and R the distance crystal–counter.

The remaining calculations are carried out in the axial system E of the elastic tensor. To this end vectors $\mathbf{V}(X_\theta Y_\theta Z_\theta)$ are transformed to the system E by means of

$$\mathbf{V}(E) = \mathbf{B}\ .\ \mathbf{U}^{-1}\ .\ \mathbf{\Phi}^{-1}\ .\ \mathbf{X}^{-1}\ .\ \mathbf{\psi}^{-1}\ .\ \mathbf{V}(X_\theta Y_\theta Z_\theta)\ . \quad (17)$$

$\mathbf{B}$ gives the transformation of $\mathbf{V}$ from the unit reciprocal axial system $\mathbf{f}^i = \mathbf{a}^i/a^i$ of the crystal to the E system, and must be supplied in the specific data of the program. The remaining matrices which serve to transform $\mathbf{V}$ from $X_\theta Y_\theta Z_\theta$ to $\mathbf{f}^i$ have been defined by Busing & Levy (1967).

To obtain an accuracy better than $1^0/_{00}$ the volume has to be divided into *ca* 1000 pyramids. This results in a computing time for each reflexion of *ca* 0·8 s for program *TDS*1 and *ca* 5 s for *TDS*2 when run on a CDC Cyber 74-16.

The programs assume an infinite resolution of the experiment (for references see under *Discussion*).

Estimation of errors due to neglect of TDS corrections

Structure models used

To estimate the errors mentioned in the *Introduction* we have used two compounds for which both the crystal structure and the elastic constants had been determined at room temperature. The compounds are dibenzoyl, DBZ, (Brown & Sadanaga, 1965; Haussühl, 1967) and ammonium hydrogen oxalate hemihydrate (Küppers, 1972, 1973). We intended to estimate the errors both at room and at lower temperatures. To obtain the latter errors models were deduced from the room temperature structures by making reasonable estimates of the thermal vibrations at lower temperatures, but by keeping cell dimensions, atomic positions and elastic tensors constant. For $T > 100$ K the parameters U_{ij} of the atoms were assumed to be proportional to T. For $T < 100$ K the thermal parameters were calculated by determining the main axes of the rigid-body translation and libration tensors at room temperature and by calculating the reduction of these tensors by means of (Keulen, 1969)

$$T_{ii}(T) = \frac{\hbar}{m\omega_i}\{[\exp(\hbar\omega_i/kT) - 1]^{-1} + 0{\cdot}5\} \quad (18a)$$

$$L_{ii}(T) = \frac{\hbar}{I\omega_i}\{[\exp(\hbar\omega_i/kT) - 1]^{-1} + 0{\cdot}5\}\ . \quad (18b)$$

For parts of the molecules which did not behave as rigid bodies the low-temperature U_{ij} values of the individual atoms were obtained from those at room temperature by multiplication with a reduction factor deduced from (18*a*) and/or (18*b*).

Influence of quantum effects

In Table 3 the $\alpha(\mathbf{H})$ values computed for both the quantum mechanical and the classical theory are compared. The table shows that for 'ordinary' measuring conditions as given in Table 2, the classical theory gives reliable $\alpha(\mathbf{H})$ values above 5 K for the compounds we have considered. Therefore the program *TDS*1 is used for the further calculations in this paper.

Table 2. *Experimental conditions*

X-rays: Mo $K\bar{\alpha}$, $\lambda = 0{\cdot}7107$ Å
Dimensions of crystal: $\varnothing = 0{\cdot}5$ mm
Mosaic spread: 0·5°
Dimensions of focus X-ray tube: 0·8 × 0·5 mm (horizontal tube)
Distance focus–crystal: 216·5 mm
Distance crystal–counter slit: 173 mm
Omega scan
Slit height: 4 mm; slit width: 3 mm
Scan range: $0{\cdot}844 + 0{\cdot}5 \tan\theta$

Errors in the atomic parameters

Let the true structure factor of the model, which we assume to consist of spherically symmetric vibrating atoms, be $F_t(\mathbf{H})$. If the errors in the observed structure amplitude are due to TDS only, this structure amplitude is given by

$$|F_o(\mathbf{H})| = |F_t(\mathbf{H})|\sqrt{1 + \alpha(\mathbf{H})}\ . \quad (19)$$

The $\alpha(\mathbf{H})$ values were calculated for the experimental conditions listed in Table 2. Thereafter block-diagonal least-squares refinements (Cruickshank, 1956) with $w = 1$ and based on $|F_o(\mathbf{H})|$ were carried out to find the changes in the parameters due to TDS. Tables 4 and 5 show the results of these refinements for different temperatures and sin θ/λ regions.

(*a*) *Coordinates.* The changes in the coordinates are small, especially at 15 K. At 293 and 110 K the changes for the heavy atoms are much smaller than the standard deviations obtained in accurate work (12×10^{-4} Å; Verschoor, 1967; Keulen, 1969). For hydrogen the systematic error due to neglect of TDS corrections is considerably smaller than the systematic errors encountered in practice because of the neglect of the deformation of the electron clouds due to chemical bonding.

(*b*) *Thermal parameters.* From (19) and (13), which show that the TDS contribution to $|F_o(\mathbf{H})|$ is proportional to $|F_t(\mathbf{H})|$ and increases with H^2, it is to be expected that neglect of TDS corrections causes the U_{ii} values to be too small. This is confirmed by Tables 4

Table 3. *Calculated α(H) values (× 10³) according to the quantum theory (Q) and classical theory (K)*

(*a*), (*b*) and (*c*) experimental conditions as in Table 2. (*d*) as in Table 2 but scan range 5°, slit height = slit width = 6 mm.

(*a*) $NH_4HC_2O_4.\frac{1}{2}H_2O$

			1 K		5 K		10 K	
h	*k*	*l*	*Q*	*K*	*Q*	*K*	*Q*	*K*
0	8	2	0	0	0	0	1	1
9	15	2	1	0	2	2	4	4
13	16	2	2	1	3	3	6	6
13	13	6	2	1	4	4	7	7
4	3	11	2	1	4	4	8	8
8	4	11	2	1	5	5	9	9
2	4	9	1	1	3	3	5	5
0	0	12	2	1	5	5	10	10

(*b*) NaCl

			1 K		5 K		10 K	
h	*k*	*l*	*Q*	*K*	*Q*	*K*	*Q*	*K*
6	6	0	1	0	1	1	2	2
10	0	0	2	0	2	2	4	4
8	8	0	3	1	3	3	5	5
5	5	5	1	0	1	1	3	2
6	6	6	2	0	3	2	4	4
10	2	0	2	0	2	2	4	4
8	2	2	1	0	1	1	2	2
6	4	4	1	0	1	1	2	2

(*c*) $C_6H_5COCOC_6H_5$

			1 K		5 K		10 K	
h	*k*	*l*	*Q*	*K*	*Q*	*K*	*Q*	*K*
0	14	1	6	3	17	16	33	32
4	12	2	7	4	18	18	36	35
9	0	20	6	4	18	18	36	36
8	2	0	1	1	5	5	10	10
12	3	0	6	3	16	15	31	31
0	0	9	0	0	1	1	2	2
0	0	27	7	4	22	22	44	44
14	0	2	6	3	17	16	33	33

(*d*) NaCl

			1 K		10 K		25 K	
h	*k*	*l*	*Q*	*K*	*Q*	*K*	*Q*	*K*
6	6	0	7	1	8	3	17	16
10	0	0	11	1	14	9	25	24
8	8	0	14	1	18	12	31	29
5	5	5	8	1	10	7	18	17
6	6	6	12	1	15	10	26	25
10	2	0	11	1	14	10	26	24
8	2	2	7	1	9	7	17	16
6	4	4	7	1	8	6	16	15

Table 4. *Results of the least-squares refinements for DBZ*

The scale factor k is defined as $kF(\text{calc}) = F(\text{exp})$. Columns 4 and 5: maximum coordinate changes; 6 and 7: average change in thermal parameters, $B = 8\pi^2 U$; 8–11: maximum change in bond lengths or angles.

			Δx_i (max) (Å)		$-10^5\Delta_{ii}$ (Å²)	$-10^3\Delta B$ (Å²)	Δl (max) (Å)		$\Delta\varphi$ (max) (°)	
(sin θ)/λ (Å⁻¹)	*k*	*R*(%)	C,O	H	C,O	H	C–C(O)	C–H	without H	with H
(*a*) 110 K										
0·0–1·0	0·9935	0·43	0·0004	0·0086	180–218	141–172	0·0005	0·0085	0·01	0·11
0·0–0·65	0·9964	0·21	0·0003	0·0037	150–175	125–150	0·0004	0·0036	0·02	0·04
0·7–1·0	0·9733	0·20	0·0001	0·0071	245–278	163–232	0·0001	0·0049	0·01	0·30
(*b*) 15 K										
0·0–1.0	0·9981	0·11	0·0000	0·0015	33–38	21–27	0·0000	0·0017	0·00	0·03
0·0–0·65	0·9993	0·04	0·0000	0·0005	22–27	18–22	0·0000	0·0006	0·00	0·01
0·7–1·0	0·9936	0·04	0·0000	0·0009	41–47	31–38	0·0000	0·0008	0·00	0·03

Table 5. *Results of the least-squares refinements for AHO*

For explanation see Table 4.

			Δx_i (max) (Å)		$-10^5\Delta U_{ii}$ (Å²)	$-10^3\Delta B$ (Å²)	Δl (max) (Å)		$\Delta\varphi$ (max) (°)	
(sin θ)/λ(Å⁻¹)	*k*	*R*(%)	C,N,O	H	C,N,O	H	C–C(O)	O(N)–H	without H	with H
(*a*) 293 K										
0·0–1·0	0·9952	0·29	0·0001	0·0033	96–201	86–142	0·0001	0·0034	0·02	0·30
0·0–0·65	0·9972	0·14	0·0001	0·0018	75–162	86–130	0·0002	0·0013	0·02	0·16
0·7–1·0	0·9799	0·21	0·0001	0·0095	127–250	61–493	0·0003	0·0153	0·01	0·26
(*b*) 110 K										
0·0–1·0	0·9971	0·17	0·0000	0·0017	40– 86	36–55	0·0000	0·0022	0·01	0·13
0·0–0·65	0·9987	0·07	0·0001	0·0024	29– 66	33–52	0·0001	0·0005	0·02	0·05
0·7–1·0	0·9899	0·10	0·0000	0·0036	53–104	30–65	0·0000	0·0024	0·01	0·19
(*c*) 15 K										
0·0–1·0	0·9995	0·03	0·0000	0·0002	6– 13	5–8	0·0000	0·0003	0·01	0·02
0·0–0·65	0·9998	0·01	0·0000	0·0001	4– 9	5–8	0·0000	0·0001	0·01	0·01
0·7–1·0	0·9983	0·02	0·0000	0·0005	5– 16	6–9	0·0000	0·0005	0·01	0·02

and 5. As the factor $1/[1+\alpha(\mathbf{H})]$ does not exactly reproduce the exponential form of a temperature factor, the scale factor is also affected. For AHO at 293 K and DBZ at 110 K the changes in the U_{ii} values of the heavy atoms are some three to nine times the standard deviation for accurate work (30×10^{-5} Å^2; Verschoor, 1967). For AHO at 110 K the changes are 1 to 4σ. At 15 K the AHO changes are less than σ while for DBZ at 15 K they are of the order of σ.

It should be noted that, although the fractional TDS contribution $\alpha(\mathbf{H})=|F_{\mathrm{TDS}}(\mathbf{H})|^2/|F_t(\mathbf{H})|^2$ is proportional to T, the absolute TDS contribution $\alpha(\mathbf{H})|F_t(\mathbf{H})|^2$ has a maximum with T as $|F_t(\mathbf{H})|^2$ decreases exponentially with T owing to the thermal vibrations of the atoms. Curves of the absolute TDS contribution have been published by Reid (1973). The temperature T(max), at which the maximum is reached, depends on the compound and on the reflexion **H** considered. T(max) decreases with increasing $\alpha(\mathbf{H})$ and lies between *ca* 30 and 200 K for different reflexions of DBZ and AHO.

Influence on difference density distributions

To check the influence of TDS on difference density distributions, three types of difference maps have been computed.

(i) A Fourier synthesis with coefficients $F_o(\mathbf{H})-F_t(\mathbf{H})$ and including all reflexions up to $\sin\theta/\lambda=1{\cdot}0$ Å^{-1}. From Fig. 3 we see that such a map, which directly shows the influence of TDS on the electron density distribution, contains high maxima at the atomic positions. Numerical data are given in Tables 6 and 7.

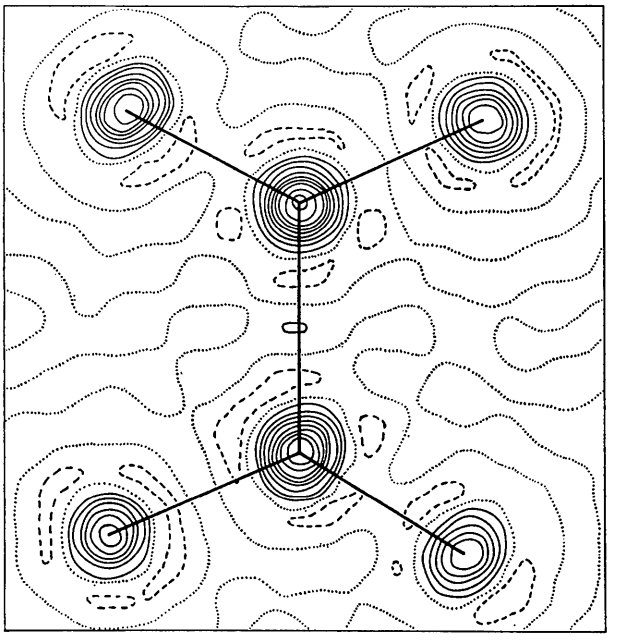

Fig. 3. Difference density in the plane of the oxalate group of AHO at 293 K for the type (i) Fourier synthesis (see text). Contours at intervals of 0·1 e Å^{-3}, ··· zero, —— positive, --- negative density.

Table 6. *Difference densities for DBZ*

(i)–(iii): Type of map (see text). For each atom D, in e Å^{-3}, is given for the atomic position (first number) and for the first diffraction ripple (second number). Columns C–C and C–O give D values at the centres of the bonds.

DBZ

	O(1)		C(1)		C(2)		C(3)		C(4)		C(5)		C(6)		C(7)		C–C	C–O
110 K																		
(i)	0·75	−0·19	1·06	−0·20	1·19	−0·19	0·96	−0·17	0·69	−0·19	0·67	−0·15	0·64	−0·15	0·85	−0·15	−0·03 to 0·09	−0·07
(ii)	0·01	−0·02	0·02	−0·03	0·01	−0·03	0·01	−0·03	0·02	−0·02	0·02	−0·02	0·02	−0·02	0·01	−0·03	0·01 to 0·03	0·02
15 K																		
(i)	0·38	−0·09	0·45	−0·08	0·47	−0·11	0·42	−0·09	0·38	−0·09	0·39	−0·08	0·37	−0·09	0·40	−0·09	0·03 to 0·05	0·00
(ii)	Flat within 0·01 e Å^{-3} except for atomic positions where $D=-0{\cdot}01$ e Å^{-3}.																	

Table 7. *Difference densities for AHO*

For explanation, see Table 6.

AHO

	C(1)		C(2)		O(1)		O(2)		O(3)		O(4)		C–C	C–O	
293 K															
(i)	0·95	−0·14	0·90	−0·16	0·80	−0·16	0·70	−0·12	0·60	−0·14	0·67	−0·14	0·11	−0·04 to	0·04
(ii)	0·01	−0·02	0·02	−0·02	0·03	−0·02	0·03	−0·02	0·03	−0·02	0·02	−0·02	0·02	0·02 to	0·03
110 K															
(i)	0·77	−0·14	0·75	−0·14	0·69	−0·15	0·70	−0·14	0·77	−0·14	0·66	−0·13	0·09	0·00 to	0·06
(ii)	0·00	−0·01	0·00	−0·01	0·00	−0·01	0·00	−0·01	0·01	−0·01	0·01	−0·01	0·01	0·02	
(iii)	0·05		0·05		0·08		0·08		0·08		0·08		0·00	0·02 to	0·03
15 K															
(i)	0·15	−0·03	0·14	−0·03	0·16	−0·03	0·15	−0·03	0·16	−0·03	0·16	−0·03	0·02	0·00 to	0·01
(ii)	Flat within 0·004 e Å^{-3} except for atomic positions where $D = -0{\cdot}004$ e Å^{-3}.														

(ii) A Fourier synthesis with coefficients $F_o(\mathbf{H})/k - F_c(\mathbf{H})$; k and $F_c(\mathbf{H})$ are the scale and calculated structure factors of a least-squares refinement based on $|F_o(\mathbf{H})|$. Both in the refinement and in the Fourier map all reflexions up to $\sin\theta/\lambda = 1{\cdot}0$ Å^{-1} are considered. At 15 K the maps are approximately flat. At 110 and 293 K there are densities of *ca* 0·03 e Å^{-3} at the centres of the bonds [*ca* 2σ for accurate work; Helmholdt & Vos (1977)]. The strong reduction of the maxima and minima in comparison with map (i) is due to the fact that the TDS errors in $F_o(\mathbf{H})$ are compensated by the change of $F_t(\mathbf{H})$ to $F_c(\mathbf{H})$ caused by the adjustment of the parameters to $|F_o(\mathbf{H})|$.

(iii) A Fourier synthesis with coefficients $F_o(\mathbf{H})/k' - F_c'(\mathbf{H})$. The scale factor k' and the parameters on which $F_c'(\mathbf{H})$ is based are obtained from a high-order ($0{\cdot}7 < \sin\theta/\lambda < 1{\cdot}0$ Å^{-1}) least-squares refinement based on $|F_o(\mathbf{H})|$ values; in the Fourier map only low-order terms up to $\sin\theta/\lambda = 0{\cdot}65$ Å^{-1} are included. This type of map is often used to study the influence of chemical bonding on electron density distributions. Only one map, for AHO at 110 K, has been calculated. From Table 7 we see that the values at the centres of the bonds are approximately the same as for map (ii), but that somewhat larger values occur at the atomic positions, from −0·02 to 0·08 e Å^{-3}. However, it is not the TDS errors at the atomic positions which are likely to spoil the study of bonding effects, as presumably larger errors occur at these positions because of small errors in scale and temperature factors.

Discussion

The error estimates in the previous section will be influenced by the approximations made in the calculation of the TDS contribution to the reflexions. For some of the approximations, *viz* (*a*) the neglect of second and higher order TDS, and (*b*) the assumption of an infinite resolution of the experiment, improvements in the programs can be made. Discussions given in the literature show, however, that the errors due to (*a*) and (*b*) tend to cancel each other. From calculations on ammonium tetroxalate (Stevens, 1974) we estimate that for this compound approximation (*a*) causes an error of −10% in the $\alpha(\mathbf{H})$ value of reflexions at $\sin\theta/\lambda = 1{\cdot}0$ Å^{-1}. From the discussions given by Cochran (1969), Jennings (1970), Walker & Chipman (1970), Scheringer (1973) and Stevens (1974) we estimate that due to approximation (*b*) our calculated $\alpha(\mathbf{H})$ values at 110 K are *ca* 10% too high at $\sin\theta/\lambda = 1{\cdot}0$ Å^{-1}.

The influence of other approximations, *viz* (*c*) the neglect of the scattering by the optic modes, and (*d*) the use of the long-wave method (see *Introduction*), is difficult to evaluate. Concerning (*c*) it is not unreasonable to assume that the TDS contributions of the optic modes are taken into account by the usual background correction. This is because for the optic modes $\omega_j(\mathbf{g})$ shows only small variations with $\mathbf{g}$ and that opposite

variations in $\omega_j(\mathbf{g})$ with $\mathbf{g}$ for different modes j will tend to eliminate variations in $\alpha(\mathbf{H}\pm\mathbf{g})$.

Larger errors may occur because of the use of the long-wave method. In the *Introduction* it has been shown that this method is valid only for small g/a^i values. For practical measuring conditions g/a^i is not always small, however. For DBZ, for instance, the maximum value of g considered in the TDS calculations is 0·037 Å^{-1} at $\sin\theta/\lambda=1{\cdot}0$ Å^{-1} which is equal to $\frac{1}{2}c^*$. (Care should thus be taken that for high $\sin\theta/\lambda$ and large unit cells, the measuring conditions are chosen such that $\mathbf{g}$ of a reflexion $\mathbf{H}$ does not point into the Brillouin zone of a neighbouring reflexion!) Stevens (1974) has made an estimate of the error due to the breakdown of the long-wave method by replacing in (6) or (7) [with $E_j(\mathbf{g})=kT$] $v_j(\hat{\mathbf{e}})\mathbf{g}$ by reasonable $\omega_j(\mathbf{g})/2\pi$ values. In this way the error in $\alpha_1(\mathbf{H}\pm\mathbf{g})$ was estimated as 10% at $\sin\theta/\lambda=1{\cdot}0$ Å^{-1}. However, (6), which is obtained from (3) and (4) by the substitution $\hat{\mathbf{U}}_j(\kappa\mathbf{g})=\hat{\mathbf{u}}_j(\hat{\mathbf{e}})$ [equation (5)] or

$$\mathbf{H}G_j(\mathbf{H}\pm\mathbf{g})=\mathbf{H}\,.\,\hat{\mathbf{u}}_j(\hat{\mathbf{e}})F(\mathbf{H})\,, \qquad (20)$$

is no longer valid if the long-wave method cannot be applied. In that case both the magnitudes and the phases of the complex quantities $\hat{\mathbf{U}}_j(\kappa\mathbf{g})$ (Cochran, 1963) will depend on κ. This implies that the first-order TDS intensity $|G_j(\mathbf{H}\pm\mathbf{g})|^2$ is no longer proportional to $|F(\mathbf{H})|^2$, but may be larger or smaller. This destroys the systematic dependence of $I_1(\mathbf{H}\pm\mathbf{g})$ on $|F(\mathbf{H})|^2$ given by (6) and it cannot be excluded that, because of this, errors will occur in the coordinates as well as in the temperature factors of the atoms if the reflexion intensities are not corrected for TDS. If the long-wave method fails the calculation of TDS errors requires the use of theoretical models for the intra- and intermolecular interactions. As long as these calculations are not available, it is best to avoid TDS as much as possible by doing the measurements at very low temperatures, say 15K.

The research has been supported by the Dutch Organization for the Advancement of Pure Research (ZWO). The computations were done at the Computing Centre of the University of Groningen.

References

BORN, M. & HUANG, K. (1968). *Dynamical Theory of Crystal Lattices*. Oxford: Clarendon Press.

BROWN, C. J. & SADANAGA, R. (1965). *Acta Cryst.* **18**, 158–164.

BUSING, W. R. & LEVY, H. A. (1967). *Acta Cryst.* **22**, 457–464.

COCHRAN, W. (1963). *Rep. Progr. Phys.* **26**, 1–45.

COCHRAN, W. (1969). *Acta Cryst.* A**25**, 95–101.

CRUICKSHANK, D. W. J. (1956). *Acta Cryst.* **9**, 747–753.

DEBYE, P. (1914). *Ann. Phys.* **43**, 49–95.

GÖTTLICHER, S. (1968). *Acta Cryst.* B**24**, 122–129.

HAUSSÜHL, S. (1967). *Acta Cryst.* **23**, 666–667.

HELMHOLDT, R. B. & VOS, A. (1977). *Acta Cryst.* To be published.

International Tables for X-ray Crystallography (1959). Vol. II, p. 264. Birmingham: Kynoch Press.

JENNINGS, L. D. (1970). *Acta Cryst.* A**26**, 613–622.

KEULEN, E. (1969). Thesis, Univ. of Groningen.

KÜPPERS, H. (1972). *Acta Cryst.* A**28**, 522–527.

KÜPPERS, H. (1973). *Acta Cryst.* B**29**, 318–327.

REID, J. H. (1973). *Acta Cryst.* A**29**, 248–251.

SCHERINGER, C. (1973). *Acta Cryst.* A**29**, 283–290.

STEVENS, E. D. (1974). *Acta Cryst.* A**30**, 184–189.

VERSCHOOR, G. C. (1967). Thesis, Univ. of Groningen.

WALKER, C. B. & CHIPMAN, D. R. (1970). *Acta Cryst.* A**26**, 447–455.

WILLIS, B. T. M. (1969). *Acta Cryst.* A**25**, 277–300.

WOOSTER, W. A. (1962). *Diffuse X-ray Reflections from Crystals*. Oxford: Clarendon Press.